Energy Broadening in the Auger-Type Neutralization of Slow Ions at Solid Surfaces

H. D. HAGSTRUM, Y. TAKEISHI,* AND D. D. PRETZER
Bell Telephone Laboratories, Murray Hill, New Jersey
(Received 19 February 1965)

Recent improved measurements of kinetic-energy distributions of electrons ejected from metals and semiconductors by slow ions make it possible to examine the energy broadening inherent in the Auger neutralization process. Broadening, defined as the full width at half maximum of a convoluting Lorentzian function, is shown in all cases to vary linearly with ion velocity for ion energies less than 100 eV. Data for He^+, Ne^+, and Ar^+ ions and the crystal surfaces Ni(111), Ge(111), GaAs(111), GaAs($\bar{1}\bar{1}\bar{1}$), and GaAs(110) show that the magnitude of broadening depends both on ion and solid and varies by a factor of 5 among the ion-solid combinations studied. For 4-eV He^+ ions the broadenings are 0.96, 0.54, 0.37, 0.17, 0.31 eV for the surfaces listed above, respectively. The velocity-dependent broadening is the sum of components due to initial-state lifetime and nonadiabatic excitation of electrons from the filled band into states above the Fermi level from which they can participate in the Auger process. Other possible broadening components—those due to final-state lifetime, energy-level shifts in the atom near the surface, and variation of surface impact parameter—are shown to be small in the low-energy range. An analysis of earlier data for He^+ on Ge(111) at ion energies up to 1000 eV indicates that the total transition rate does not increase appreciably above 100 eV, most likely as a result of the collapse of the barrier between the ion and the solid at higher ion energies. This analysis also shows that nonadiabatic excitation accounts for at most 1/3 and initial-state lifetime for at least 2/3 of the broadening at energies below 100 eV. The initial-state-lifetime broadening thus deduced shows the Auger neutralization process to be very rapid, having a transition rate for 4-eV He^+ ions on Ge(111) of about 5×10^{14} sec^{-1}. The magnitude deduced for broadening due to nonadiabatic excitation is shown to be in the range expected. Possible reasons for the variation with ion and solid are suggested also.

I. INTRODUCTION

OUR understanding of an electronic transition process is incomplete without knowledge of the source and magnitude of the energy broadening inherent in it. In the present work we have studied the energy broadening of the Auger-type process in which electrons are ejected from a solid when ions of sufficiently large neutralization energy are neutralized at the solid surface. The two electronic transitions involved are indicated on the electron energy-level diagram of Fig. 1.

For a given ion-target combination the process is studied experimentally by measuring total yield and kinetic-energy distribution of the ejected electrons as functions of incident-ion kinetic energy. The form of the distribution changes as incident-ion energy is increased for reasons which have been understood to be connected with the energy broadening of the neutralization process.[1–5] A number of possible sources of broadening have been recognized and discussed in earlier work, but only preliminary attempts have been made at the quantitative measurement of broadening and the assignment of relative magnitudes to the various broadening components.[4,5]

Recent improvements in experimental techniques enable us to measure electron kinetic-energy distributions at lower incident-ion energies than in earlier work.[6] We have also improved the relative accuracy of distributions measured at closely spaced ion energies. These advances now make possible a quantitative study of energy broadening in the Auger neutralization process. Data have been accumulated recently on several monocrystalline materials, both metals and semiconductors, using the ions He^+, Ne^+, and Ar^+. In particular, the results obtained for the (111) face of nickel,[7] the (111) and (100) faces of Ge,[8] and the (111), ($\bar{1}\bar{1}\bar{1}$), and (110) faces of GaAs[9] are used in this paper. We restrict ourselves to atomically clean and annealed surfaces.

In this paper we first determine the magnitude and velocity dependence of the experimentally observed broadening (Sec. II). Next the possible broadening components are discussed (Sec. III) and their magnitudes estimated for various energy ranges (Sec. IV). Possible reasons for the observed variation in broadening with ion and solid are suggested (Sec. IV) and some conclusions concerning the barrier between atom and solid are drawn (Sec. V).

---

* Present address: Central Research Laboratory, Toshiba Electric Company, Kawasaki, Japan.

[1] H. D. Hagstrum, Phys. Rev. **96**, 325 (1954), polycrystalline W; **104**, 672 (1956), polycrystalline Mo.

[2] F. M. Propst and E. Lüscher, Phys. Rev. **132**, 1037 (1963), polycrystalline W.

[3] H. D. Hagstrum, Phys. Rev. **119**, 940 (1960), monocrystalline Ge and Si.

[4] H. D. Hagstrum, Phys. Rev. **96**, 336 (1954).

[5] H. D. Hagstrum, Phys. Rev. **122**, 83 (1961).

[6] H. D. Hagstrum, D. D. Pretzer, and Y. Takeishi, Rev. Sci. Instr. (to be published).

[7] Y. Takeishi and H. D. Hagstrum, Phys. Rev. **137**, A641 (1965), Ni(111).

[8] Y. Takeishi and H. D. Hagstrum, Surface Sci. **3**, 175 (1965), Ge(111), (100).

[9] D. D. Pretzer and H. D. Hagstrum (to be published); GaAs(111), ($\bar{1}\bar{1}\bar{1}$), (110).

II. MAGNITUDE AND VELOCITY DEPENDENCE OF BROADENING

The experimental data on which the conclusions of this paper are based are the families of kinetic-energy distributions $N_0(E)$ of electrons ejected by noble-gas ions of various incident kinetic energies K. Figures 2 and 3 show such data for He^+ ions incident on the atomically clean faces of Ni(111)[7] and Ge(111),[8] respectively. These are tracings of X-Y recorder plots of the analog derivative of electron collector current

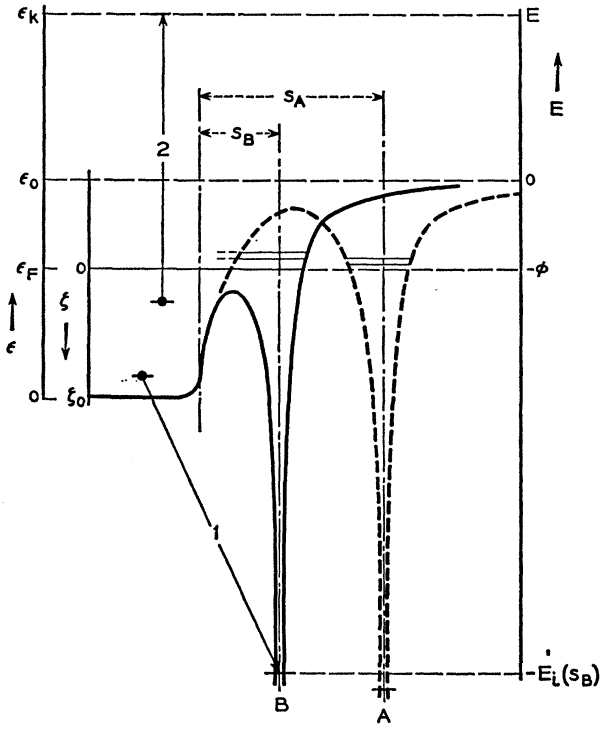

FIG. 1. Electron energy diagram for the Auger neutralization process showing the ion at two positions (A and B) outside a metal at distances s_A and s_B from the surface. Electron transitions are shown as arrows 1 and 2 originating in the filled band of the metal at the left. Excited states of the atom are indicated just above the Fermi level. Energies and energy scales are defined by the figure. The ϵ scale (positive up) is zero at the bottom of the filled band. ζ (positive down) is zero at the Fermi level for a metal. For a semiconductor, $\zeta=0$ at the top of the valence band which occurs at ϵ_0 on the ϵ scale. E (positive up) is the energy outside the solid and is zero at the vacuum level.

versus retarding potential.[6] Note that data are available for ions having incident energies as low as $K=4$ eV. Significant differences in $N_0(E)$ are observed for changes in K of 1 eV. Similar data are available for Ne^+ and Ar^+ ions, and for other target faces as already indicated. Recent data have been taken to K values no greater than 100 eV. Earlier data for polycrystalline W and Mo[1] and for monocrystalline Ge and Si[3] were obtained for K values up to 1000 eV and are used in this paper also.

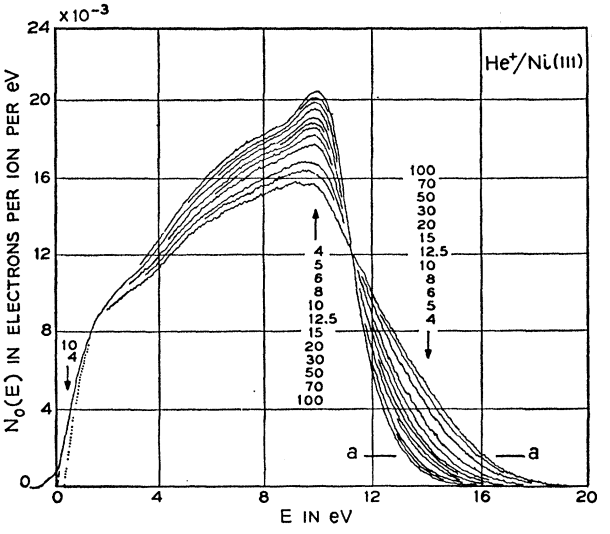

FIG. 2. Experimental kinetic-energy distributions for He^+ ions incident on atomically clean Ni(111). Incident-ion kinetic energies K in electron volts are indicated in sequence at three points on the curves. The level $N_0(E)=1.5\times10^{-3}$ electrons/ion/eV is indicated by the line a-a.

Energy broadening manifests itself in the experimental data, like Figs. 2 and 3, as an increase in the extent of the high-energy tail of the distribution and a smearing out of its structural features as ion energy increases. We can attribute these observed features to energy broadening of the Auger neutralization process only if no other competing processes occur. There are three possible competing processes whose roles must be

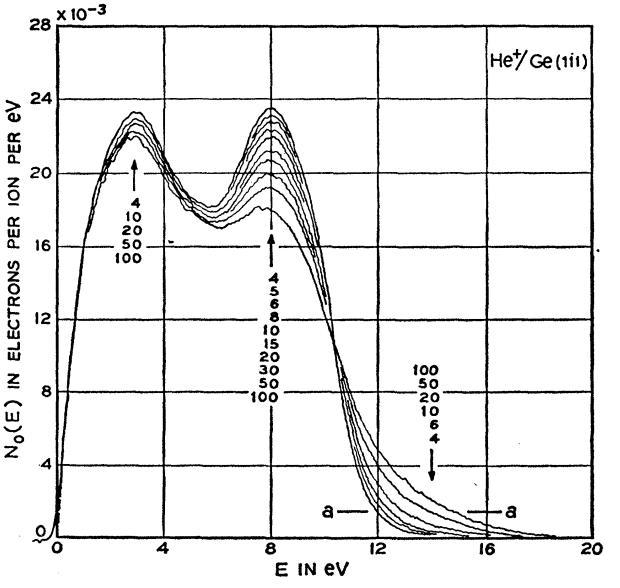

FIG. 3. Experimental kinetic-energy distributions for He^+ ions on atomically clean Ge(111). K values in electron volts are indicated in sequence at three points on the curves. Line a-a indicates $N_0(E)=1.5\times10^{-3}$ electrons/ion/eV.

assessed: (1) Kinetic ejection of electrons by direct interaction of the ion or neutralized atom with electrons of the solid. As shown in the Mo work,[1] electrons from this process begin to appear at ion energies of several hundred electron volts and have considerably smaller kinetic energies than the Auger electrons. Thus they would not affect the higher energy portions of the Auger distributions. (2) Possible secondary emission by the faster Auger electrons.[10,11] To the extent that such electrons appear they will also be in the low-energy end of the distribution. (3) Auger de-excitation[4] in which the excited states of the incoming atom are partially populated by electrons from the solid. This is an important consideration in this paper and is discussed in Sec. IV.

For quantitative discussion we need a single parameter which characterizes the broadening of a particular kinetic-energy distribution. We shall use two such parameters in this paper. The first z is defined as the distance on the energy scale from the position of the maximum of the distribution to the curve itself at a level fh, a specified fraction f of the total height h of the main peak of the distribution. We shall call z the "extension" of the $N_0(E)$ distribution. In this work we have used the values $f=0.05$ and 0.08, designating the corresponding extensions as z_5 and z_8, respectively. These parameters are indicated on the $N_0(E)$ distribution of Fig. 4.

It can be shown that changes in z will be approximately proportional to changes in the energy broadening. As in earlier work[4,5] we shall assume that energy broadening is introduced into the theory by the convolution of the internal electron distribution $N_{i0}(E)$ by a broadening function. Thus the internal distribution at energy K_2, $N_{iK_2}(E)$, is related to the distribution at $K_1(<K_2)$,$N_{iK_1}(E)$, by the relation

$$N_{iK_2}(E)=\int_{-\infty}^{\infty} B(x,L_{K_1K_2})N_{iK_1}(E-x)dx. \qquad (1)$$

Here $B(x,L_{K_1K_2})$ is the broadening function and $L_{K_1K_2}$ is the parameter which specifies its width. The externally observed distribution $N_0(E)$ for ion energy K is obtained by multiplying $N_{iK}(E)$ by a suitable probability of electron escape over the surface barrier, $P_e(E)$.[4,5] Since $P_e(E)$ will vary relatively slowly for $E>5$ eV the results of the convolution of Eq. (1) should be relatively apparent in $N_0(E)$ for $E>5$ eV. For $E\leq 5$ eV $P_e(E)$ will affect the form of $N_0(E)$ and, for this reason, we expect some quantitative uncertainty in the results for Ar^+.

If in (1) we make $N_{iK_1}(E)=1$, $E<E_1$; 0, $E>E_1$ and for $B(x,L_{K_1K_2})$ take the Lorentzian:

$$B(x,L_{K_1K_2})=(L_{K_1K_2}/\pi)/(L_{K_1K_2}{}^2+x^2). \qquad (2)$$

The extension $z=E-E_1$ at the level f in the convoluted distribution $N_{iK}(E)$ turns out to be

$$z=E-E_1=L_{K_1K_2}\tan(\tfrac{1}{2}\pi-f\pi). \qquad (3)$$

Since $2L_{K_1K_2}$ is the total width at half-maximum of the broadening function usually taken as the energy broadening b, we have shown for this special case that the extension z is proportional to broadening. For any

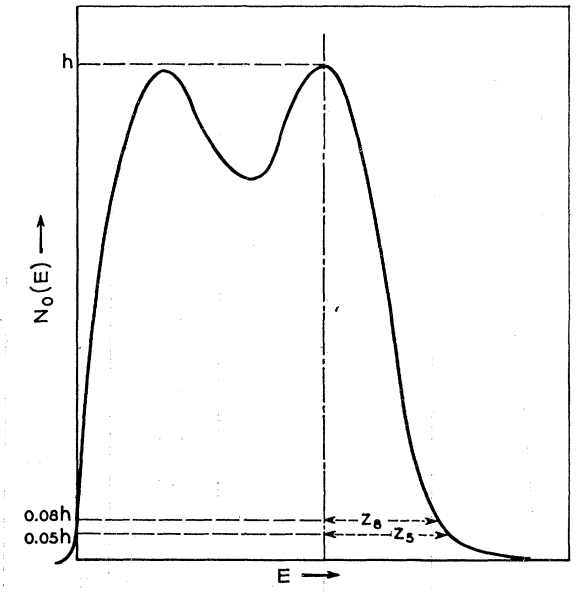

FIG. 4. Diagram illustrating the definitions of the relative extensions z_5 and z_8 used to provide a measure of the relative broadening in the electron kinetic-energy distributions.

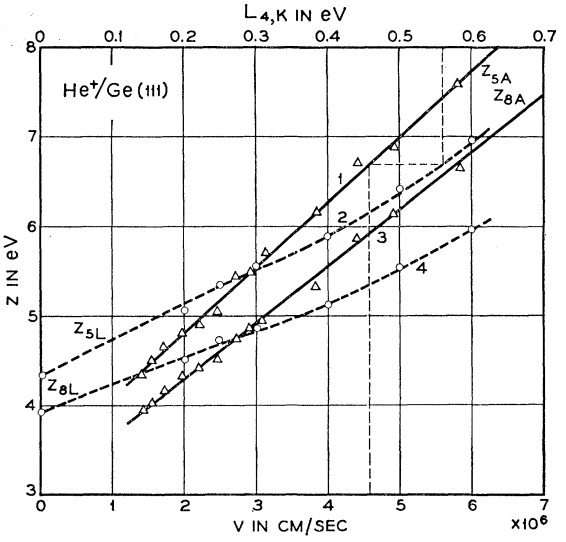

FIG. 5. Plots of z_{5A} and z_{8A} versus v, curves 1 and 3, and of z_{5L} and z_{8L} versus L_{4K}, curves 2 and 4, for He^+ on Ge(111). The procedure for finding the relation between L_{4K} and v by reading L_{4K} and v on the appropriate curves at the same value of z is illustrated by the broken dashed line.

[10] F. M. Propst, Phys. Rev. **129**, 7 (1963).
[11] H. D. Hagstrum and Y. Takeishi, Phys. Rev. **137**, A304 (1965).

$N_{iK}(E)$ which has a reasonably sharp cutoff at its high-energy end we expect changes in z, Δz, to be proportional to changes in broadening. We recognize that not all the energy broadening components can be represented by a Lorentzian but in general the definition of Δz as a measure of incremental broadening appears reasonable.

We proceed to determine the magnitude of the velocity-dependent broadening components in the case of He^+ ions on Ni(111) and Ge(111). We assume Eq. (1) applies and shall use a Lorentzian broadening function [Eq. (2)]. In this discussion a Lorentzian parameter with two subscripts, as $L_{K_1K_2}$, is understood to indicate the parameter of the Lorentzian which will broaden the $N_0(E)$ distribution at ion energy K_1 into that at K_2. The application of successive convolutions having parameters $L_{K_1K_2}$ and $L_{K_2K_3}$ is equivalent to a single convolution with the parameter $L_{K_1K_3}$ given by

$$L_{K_1K_3}=L_{K_1K_2}+L_{K_2K_3}. \quad (4)$$

The use of two levels $f=0.05$ and 0.08 serves as a check on whether the Lorentzian reasonably represents the convoluting function. These values of f lie sufficiently far apart so that their difference is significant and yet are both small enough so that the difference in z between curves is sufficiently large to be measured with reasonable accuracy.

Our goal here is to determine a Lorentzian broadening parameter L_{0K} which characterizes the velocity-dependent broadening at ion energy K and to be able to plot this as a function of ion velocity. Four steps are necessary to achieve this:

(1) We measure the extensions z_5 and z_8 directly on experimental analog plots of $N_0(E)$ like those of Figs. 2 and 3. We call these parameters z_{5A} and z_{8A} to distinguish them from another set defined in step (2). We can than plot these parameters as functions of ion velocity as is done for He^+ on Ge(111) in Fig. 5, curves 1 and 3. We use nominal velocity of the ion calculated from ion energy at large distances from the surface and thus neglect the acceleration due to image force attraction near the surface.

(2) Next, in a machine calculation, we broaden the experimental $K=4$-eV distribution by convoluting with a series of Lorentzian functions of increasing parameter L_{4K}. We now measure the extensions z_{5L} and z_{8L} on these calculated distributions. These are plotted versus L_{4K} as curves 2 and 4 in Fig. 5 for He^+ on Ge(111).

(3) With z_A plotted against v and z_L plotted against L_{4K} it is now possible to obtain a relation between L_{4K} and v. Corresponding values of v and L_{4K} are obtained by reading v from curve 1 (or 3) of Fig. 5 at a given z and L_{4K} from curve 2 (or 4) at the same value of z. The v values used were those at which $N_0(E)$ distributions had been measured but the intermediate z values were read from the smooth curves passed through the data points. This gives us L_{4K} versus v which is plotted for He^+ on Ge(111) in Fig. 6. Data from $f=0.5$ and $f=0.8$ are seen to fall on the same curve. Similar results obtained by the procedure described above for the Ni(111) data of Fig. 2 are shown in Fig. 7. We see

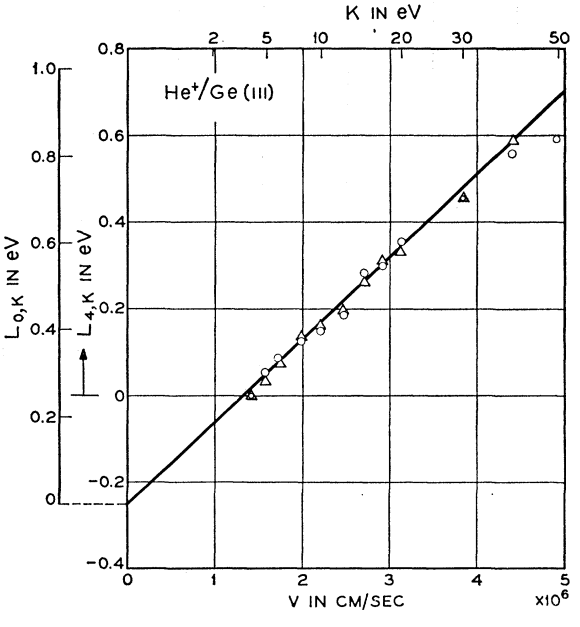

FIG. 6. Plot of Lorentzian parameter L_{4K} versus ion velocity for He^+ on Ge(111). Data for $f=0.05$ are shown as circles, those for $f=0.08$ as triangles. Extrapolation to $v=0$ defines the L_{0K} scale as discussed in the text.

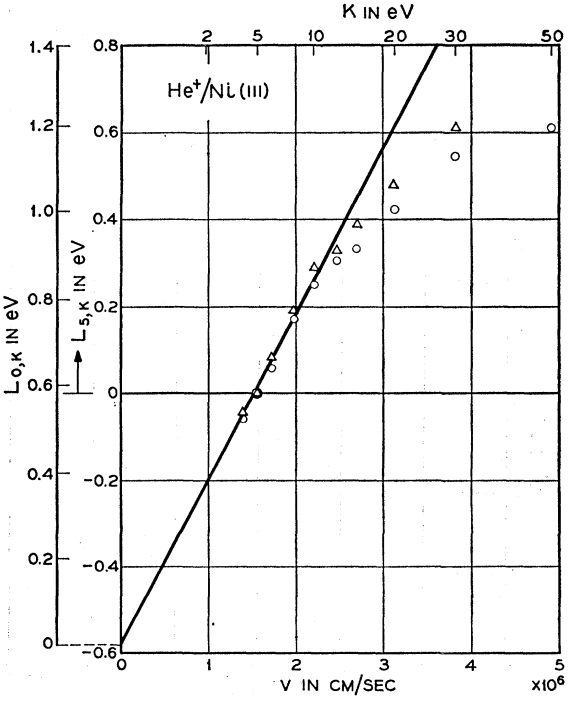

FIG. 7. Plots of Lorentzian parameters L_{5K} and L_{0K} versus v for He^+ on Ne(111). Circles $f=0.05$, triangles $f=0.08$.

that in each case the incremental broadening beyond $K=4$ or 5 eV varies linearly with velocity at the lower ion velocities.

(4) Finally, we extrapolate the linear portions of these plots to $v=0$ to obtain an L_{0K} scale giving the total velocity-dependent broadening $b=2L_{0K}$ at ion energy K. This assumes, as discussed further in Sec. V, that the variation in barrier thickness responsible for the principal variation with v does not otherwise greatly distort the $N_0(E)$ distributions in the range of v over which we have data. Total broadening at ion energy $K<100$ eV will include small contributions from broadening components which are independent of velocity (Sec. IV).

To facilitate convenient comparison of broadenings for different targets and ions we define a second extension parameter z' as the energy distance from a specially chosen zero to the high-energy tail of the distribution measured at the level $N_0(E)=1.5\times10^{-3}$ electons/ion/eV, irrespective of the total height of the distribution. This level of $N_0(E)$ is indicated in Figs. 2 and 3. For He^+ ions it lies in the range $f=0.05$ to 0.08. Since it is really dz'/dv that is significant the zero of z' is chosen so that the linear extrapolation of z' with v passes through $z'=0$ at $v=0$.

Data of z' versus v for He^+ ions on several target faces are shown in Fig. 8 and for three different ions on Ge(111) and Ni(111) in Fig. 9. Initial slopes, dz'/dv for these and similar data are tabulated in Table I.

The data on broadening given above are restricted to ion energies K below 100 eV. For K much higher than this the main peak of the distribution becomes quite broad or disappears entirely making it impossible to determine the zero of z. The measurement of z' for $K>100$ eV is affected by several factors which will be evaluated in Sec. IV after the nature of the broadening components have been discussed in Sec. III. Measurement z' has been extended beyond $K\sim100$ eV using the original data of earlier work on Ge(111) (Exp. 28) in which ion energies to 1000 eV were used.[3] Curves 1 and 3 of Fig. 10 give such data for He^+ and Ne^+ ions. The initial slopes indicated by the dashed lines are from the later measurements (Exp. 30) plotted in Figs. 8 and 9 and tabulated in Table I. Note the good agreement between the two experiments.

In connection with Figs. 5, 6, and 7 we arrived at a quantitative measure of broadening b as the width at half-maximum of the broadening function $B(x,L_{K_1K_2})$ of Eq. (1). If $B(x,L_{K_1K_2})$ is the Lorenztian of Eq. (2), $b=2L_{0K}$ as we have seen. We may also relate the extension parameter z' to the broadening b using the

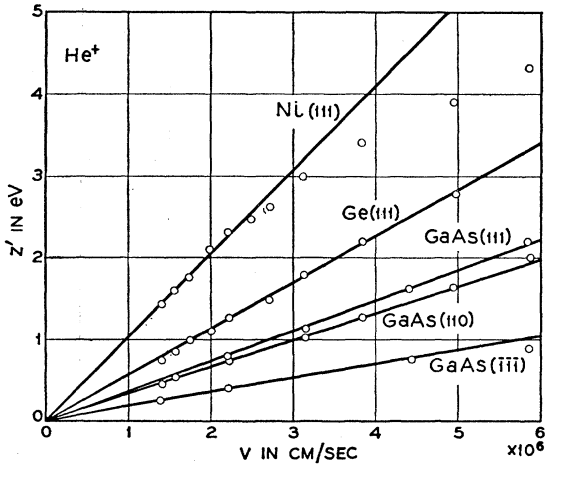

FIG. 8. Plots of z' versus v for He^+ ions incident on various clean monocrystalline surfaces.

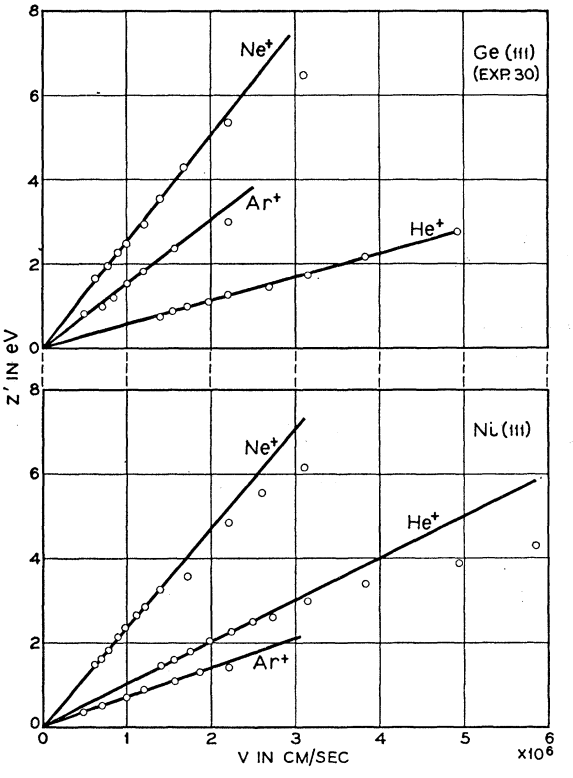

FIG. 9. Plots of z' versus v for He^+, Ne^+, and Ar^+ ions on Ge(111) and Ni(111).

He^+/Ge(111) data of Figs. 6 and 8. From the initial slopes in these figures, which result from the same broadening components, we obtain $dL_{0K}/dv=0.19\times10^{-6}$ eV cm^{-1} sec and $dz'/dv=0.57\times10^{-6}$ eV cm^{-1} sec. Thus

$$b=2L_{0K}=0.67z'. \tag{5}$$

b, and hence L_{0K}, in this case involves more than one broadening component.

III. BROADENING COMPONENTS

There are five types of energy broadening operative in the Auger neutralization process. These result from:

(1) initial-state lifetime,
(2) final-state lifetime,
(3) shift in atomic energy levels near the surface,
(4) variation of impact parameter at the surface,
(5) nonadiabatic excitation of electrons in the solid as the result of the ion's motion.

The first four causes of broadening have been recognized before.[4,5] The last, suggested as a possiblity by Herring,[12] has not been considered previosuly in connection with ion neutralization processes. We shall discuss these broadening components in order and attempt to assess their magnitude and their dependence on ion velocity. We assign to each a broadening parameter b according to the scheme of Table II.

Initial-state lifetime broadening b_i arises via the

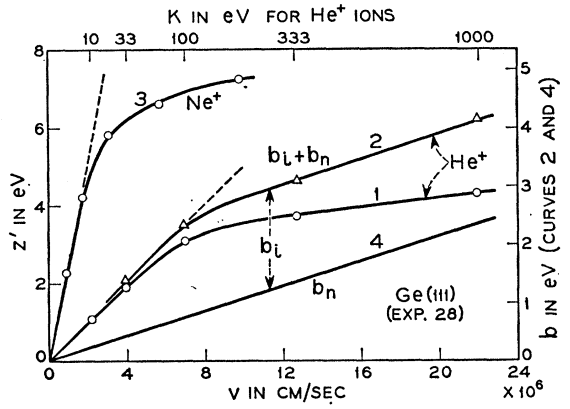

FIG. 10. Plots of z' versus v for He^+ (curve 1) and Ne^+ (curve 3) on Ge(111) from earlier work. Curve 2 is a correction of curve 1 to include the effects of variation of effective neutralization energy, $E_i(s_t)$, as discussed in the text. Curve 2 thus also represents (b_i+b_n) on the scale of b at the right. Curve 4 is an estimate of an upper limit for b_n.

Heisenberg uncertainty principle and is written

$$b_i=\hbar/\tau_i=\hbar R_t(s_t)\,, \tag{6}$$

where τ_i is the initial-state lifetime and $R_t(s_t)$ is the total transition probability per unit time with the ion at the distance from the surface s_t at which the electronic transitions occur. For a sufficiently thick barrier we expect an exponential or nearly exponential rate function:

$$R_t(s)=A\,\exp(-as)\,. \tag{7}$$

It was shown earlier[4,5] that this leads to a probability $P_t(s,v)$ that an ion of velocity v is neutralized in ds at s having the form

$$P_t(s,v)=(A/v)\,\exp[-(A/av)\,\exp(-as)-as]\,. \tag{8}$$

The transition distance s_t is approximately equal to the distance s_m at which P_t is maximum:

$$s_t\cong s_m=(1/a)\,\ln(A/av)\,. \tag{9}$$

Under these conditions initial-state lifetime broadening, b_i will be

$$b_i=\hbar av \tag{10}$$

and the corresponding transition rate

$$R_t=av\,. \tag{11}$$

In earlier work[4,5] estimates of $a\sim 3$ Å^{-1} were obtained by considering wave-function tails and the distance dependence of interaction potentials in solids. This value for a gives $b_i\sim 0.3$ eV, $R_t\sim 4\times10^{14}$ sec^{-1} for 4-eV He^+ ions ($v=1.4\times10^6$ cm/sec); and $b_i\sim 4$ eV, $R_t\sim 7\times10^{15}$ sec^{-1} for 1000-eV He^+ ions ($v=21.9\times10^6$ cm/sec). As is discussed in Sec. IV, it is probable that the transition rate does not reach such high values as those calculated from Eq. (10) for 1000-eV ions because the barrier between ion and solid collapses. Initial-state lifetime must be considered a major contributor to the observed broadening, however. We present a more detailed evaluation of its magnitude in Sec. IV.

Of the five components of broadening listed only that due to final-state lifetime is independent of incident-ion velocity and must be less than or equal to the total experimental broadening observed for the slowest ions. Furthermore, it is dependent on the energy of the holes left in the band of the solid, and increases with increasing ζ, the energy measured down from the top of the band.[13] In metals the final-state lifetime broadening is zero at the Fermi level ($\zeta=0$) and in semiconductors at $\zeta=E_g$, a distance down into the band equal to the width of the forbidden energy gap.

TABLE I. Values of dz'/dv for various surfaces and ions.

	$10^6\times dz'/dv$ in eV cm^{-1} sec		
	He^+	Ne^+	Ar^+
Ni(111)	1.02	2.33	0.72
Ge(111)	0.57	2.52	1.54
Ge(100)	0.59	2.91	1.52
GaAs(111)	0.39	2.30	1.55
GaAs($\bar{1}\bar{1}\bar{1}$)	0.18	1.00	0.70
GaAs(110)	0.33	1.75	1.30

TABLE II. Energy-broadening components.

Symbol	Source of broadening
b_i	initial-state lifetime
b_f	final-state lifetime
b_a	atomic level shifts
b_s	surface impact parameter
b_n	nonadiabatic excitation

[12] C. Herring (private communication). See also C. Herring, in *Proceedings of the Photoconductivity Conference*, edited by R. G. Breckenridge (John Wiley & Sons, Inc., New York, 1956).

[13] H. W. B. Skinner, Phil. Trans. Roy. Soc. (London) **A239**, 95 (1940); P. T. Landsberg, Proc. Phys. Soc. (London) **A62**, 806 (1949).

A principal means of estimating broadening due to final-state lifetime comes from mean free paths of hot electrons in solids. We may use such data for holes since scattering mean free paths of equally energetic holes and electrons are comparable.[14] Bartelink, Moll, and Meyer[15] have provided new determinations of electron mean free paths in silicon and compared them with the earlier theoretical estimates of Wolff and Shockley based on avalanche breakdown. Their shortest mean free path for electrons excited by 4- to 5-eV is 60 Å for optical-phonon interaction. Gobeli and Allen[16] have obtained a mean free path of 25 Å for photoelectrons of comparable energy for all types of inelastic *and elastic* scattering processes. It should thus be a lower bound for inelastic processes. Quinn[17] has calculated a mean free path of 75 Å for electrons excited by 5 eV in aluminum. Thus in either metals or semiconductors we conclude that the mean free path of electrons and hence holes is of the order of 50 Å about 5 eV from the band edge. Taking the hole velocity to be in the range 10^{15} to 10^{16} Å sec^{-1} we obtain a final-state lifetime in the range 5×10^{-14} to 5×10^{-15} sec which corresponds to a final-state lifetime broadening in the range 0.013 to 0.13 eV. These numbers are corroborated by the resolution of 0.1 eV or less found in the kinetic-energy spectra of photoelectrons 4 eV above the bottom of the conduction band in semiconductors.[18] We conclude from the above that the final-state lifetime broadening b_f in either metals or semiconductors is of the order of 0.1 eV or less for Auger neutralization processes having final-hole states lying within 4 to 5 eV of the top of the filled band. We recall that it starts from zero at $\zeta=0$ for metals and $\zeta=E_g$ for semiconductors and thus should be negligible over the top several electron volts of the band.

It is also possible to eliminate components (3) and (4) as possible contributors to the broadening observed for ions in the energy range $K \lesssim 100$ eV. We may best understand the broadenings due to energy level shifts and the variation of surface impact parameter in terms of the potential-energy diagram of the system of ion and solid shown in Fig. 11, discussed extensively elsewhere.[4] Since the Franck-Condon principle holds, the Auger process occurring at a given distance s_t is represented in Fig. 11 by a vertical transition from the initial state, curve 1, to some final state represented by a curve lying between curves 2 and 3. Final states differ in energy by virtue of the different energy levels in the solid from which the participating electrons may be taken. The kinetic energy of the ejected electron outside the solid is the vertical distance at s_t between the initial- and final-state potential curves. Its maximum value is $E_i(s_t)-2\varphi$ as shown in the figure. $E_i(s_t)$ is the effective neutralization energy of the ion at the distance of transition s_t and φ is the work function of the metal. From this value the variation of $E_i(s)$ may be estimated. A curve of the incremental change $\Delta E_i(s)=E_i(\infty)-E_i(s)$ from previous work[4] is reproduced as curve 1 of Fig. 12.

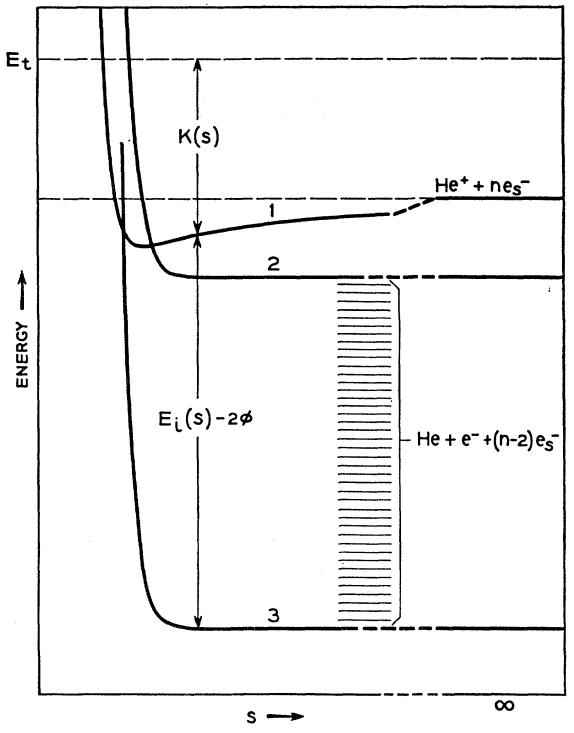

FIG. 11. Potential-energy diagram showing the variations of initial and final states of the Auger neutralization process as functions of distance of the atomic species from the solid surface. E_t is the total energy of the system, both potential and kinetic. $K(s)$ is the ion kinetic energy, $E_i(s)$ is the ion neutralization energy, each at the distance s. φ is the work function of the metal.

Level shift broadening comes about because $E_i(s)$ is not a constant. Thus if the Auger process occurs over a range of distances Δs, level shift broadening is proportional to $[dE_i(s_t)/ds]\Delta s$. We note from Fig. 12 the important fact that this quantity cannot increase unless $E_i(s)$ itself decreases. Decrease in $E_i(s)$ shifts the $N_0(E)$ distribution to lower E. Further it is apparent that this broadening cannot produce faster electrons at higher ion energy K than are produced at lower K. Since the experimental data of Figs. 2 and 3 indicate very little shift in the maxima of $N_0(E)$ as K increases we cannot attribute the broadening in the range $K<100$ eV to energy-level shifts.

Variation of impact parameter relative to a surface atom [Type (4)] has been discussed in connection with Fig. 28 of Ref. 5. It may be accounted for by making the position of the $\Delta E_i(s)$ curve of Fig. 12 depend on impact

[14] C. A. Lee, R. A. Logan, R. L. Batdorf, J. J. Kleimack, and W. Wiegmann, Phys. Rev. **134**, A761 (1964).
[15] D. J. Bartelink, J. L. Moll, and N. I. Meyer, Phys. Rev. **130**, 972 (1963).
[16] G. W. Gobeli and F. G. Allen, Phys. Rev. **127**, 141 (1962).
[17] J. Quinn, Phys. Rev. **126**, 1453 (1962).
[18] G. W. Gobeli, F. G. Allen, and E. O. Kane, *Proceedings of the Seventh International Conference on the Physics of Semiconductors, Paris, 1964* (Dunod Cie., Paris, 1964), p. 937.

parameter. Curves 1 and 2 in Fig. 12 indicate schematically the limits of variation over the surface. This effect broadens the distributon but will have the same characteristics with respect to ion velocity as does the level shift broadening and cannot thus be operative at low ion energies. $[dE_i(s)/ds]\Delta s$ will be sufficiently small if the process occurs where $dE_i(s)/ds$ is not extremely large, i.e., outside the range where repulsive forces become appreciable and if the transition rate is high enough to keep Δs small. From the relative constancy in position of the peaks of the $N_0(E)$ distributions at small K we estimate (b_f+b_s) to be of the order of 0.1 eV or less for $K<100$ eV. Above $K\sim100$ eV $N_0(E)$ shifts to lower energy indicating that b_s increases. This will smear $N_0(E)$ even though faster electrons than at lower K cannot be produced.

The transfer of kinetic energy from the ion to the electrons of the solid is not essential to the unbroadened Auger neutralization process. The process is resonant and could in principle proceed with high probability in the adiabatic region for a stationary ion outside the solid surface. However, in the interaction of a moving ion with a solid nonadiabatic excitations of the electrons of the solid are possible. The system of moving ion and solid cannot remain in its ground state. Electrons excited to states above the normally filled states in the solid can participate in the Auger process and yield faster electrons than would otherwise be observed. Such excitation into higher states and the depletion of lower states can be shown to have the same general effect on an electron distribution as does convolution by a broadening function [Eq. (1)].

Consider the frequency spectrum of the electric potential at the position of an electron near the moving ion. Fourier analysis of the potential at a point which lies a distance d from the line of motion of the ion yields the results

$$F(\omega)=\int_{-\infty}^{\infty} q^2(d^2+v^2t^2)^{-1/2}\exp(-i\omega t)dt$$
$$=2(q^2/v)K_0(\omega d/v), \qquad (12)$$

where q is the ionic charge, v the ion velocity, and $K_0(\omega d/v)$ is the modified Bessel function of the argument $(\omega d/v)$. Using the asymptotic form $(\pi/2x)^{1/2}\times\exp(-x)$ for $K_0(x)$ which deviates appreciably from $K_0(x)$ only for $x<0.3$ we may write

$$F(\omega)=[(2\pi)^{1/2}q^2/(\omega v d)^{1/2}]\exp(-\omega d/v). \qquad (13)$$

We expect that the probability of an excitation of amount $(\Delta E)=\hbar\omega$, occurring at d, proportional to $F^2(\omega)$. At sufficiently large ω the exponential term will dominate the pre-exponential factor. Thus the combination of variables in the exponential, $(\omega d/v)=[(\Delta E)d/\hbar v]$ indicates that (ΔE) should be proportional to v. The magnitude of $F(\omega)$ will be appreciable only if the argument of K_0 in Eq. (12) is of the order of unity. This leads to an expression for nonadiabatic broadening:

$$b_n=(\Delta E)\sim\hbar v/d. \qquad (14)$$

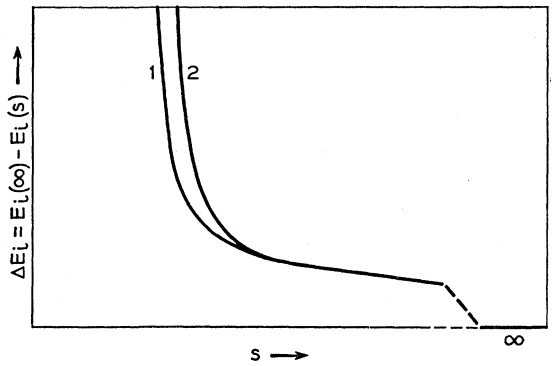

FIG. 12. Schematic variation of the change in ion neutralization energy with distance from the solid surface. Curves 1 and 2 indicate the extremes of the dependence caused by changing the impact parameter of the incident ion relative to a surface atom.

Screening by electrons of the solid will limit d to less that 1 Å if the density of electrons at the ion position is close to that in the bulk. b_n varies as $1/d$ but the number of electrons available for excitation by the moving ion varies as d^n ,where n has a value between 2 (cylinder) and 3 (sphere). Thus reduction of d to increase b_n reduces the probability that the effect occurs at all. If we take $d\sim0.5$ Å we find $b_n\sim0.2$ eV for 4 eV, He^+ ions, ~3 eV for 1000 eV, He^+ ions. b_n should thus be comparable in magnitude to b_i.

Herring's work on nonadiabatic effects related to traps[12] indicates that an expression like (13) gives the electronic excitation arising from nuclear motion if d is interpreted as the nuclear displacement over which the electronic wave functions vary appreciably. Herring considers 0.5 Å as a reasonable number for such a distance. Equation (13) is also of the form of the adiabatic criterion introduced by Massey[19] in the study of atomic collisions.

Finally, we point out that the density as well as the character of the final states into which electrons are nonadiabatically excited should effect the magnitude of nonadiabatic broadening. In metals these could be the unoccupied but available states immediately above the Fermi level. In semiconductors the only states available immediately above the filled valence band are the states in the energy gap at the surface. These surface states are most likely indistinguishable at the ion position, except for possible density differences, from valence-band states. The incoming atom also provides empty excited states which for the noble gases lie in the energy region of interest (see Fig. 1). These states vary in energy for the different atoms and with distance of the atom from the surface.[4] They become broadened virtual bound states for metals since they interact with

[19] H. S. W. Massey, Rept. Progr. Phys. **12**, 248 (1949).

allowed levels of the same energy in the solid.[20] For semiconductors they will remain discrete if they remain in the forbidden energy gap and there are no surface states. Interaction with surface states should transform the excited states to virtual bound states as in the case of metals. Nonadiabatic excitation into these excited states, which should be very effective in broadening an Auger energy distribution because of the large wave-function overlap between them and the atomic ground state, may well account for the observed dependence of broadening on the nature of the solid and the ion.

IV. RELATIVE MAGNITUDE OF BROADENING COMPONENTS

In this section we shall present the evidence that contributes to an assessment of the relative magnitudes of the broadening components. For He^+ ions of energy $K<100$ eV incident on Ge(111) and Ni (111) we have seen that the incremental broadening varies linearly with velocity and have determined its magnitude. We have also seen that in this energy range only two of the five possible broadening components are expected to be velocity dependent and of sufficient magnitude to account for these observations. Thus we conclude that in this energy range

$$(b_i+b_n)=0.67(dz'/dv)v, \tag{15}$$

using Eq. (5). The data of Table I may be used to evaluate (b_i+b_n) for each of the ion-target combinations studied. Reasons for believing that this procedure overestimates (b_i+b_n) for Ne^+ are discussed below. Values of (b_i+b_n) are given in Table III for He^+ ions and are more accurate than the estimated values of its components.

The estimates given of b_i and b_n in Sec. III suggest that the measured (b_i+b_n) is neither all b_i nor all b_n. Experimental observation of $N_0(E)$ indicates that the Auger neutralization process still occurs in recognizable form at $K=1000$ eV for He^+ ions. Although the number of ions reflected as ions or metastables has increased and electrons from kinetic ejection are present in $N_0(E)$ at this energy[1] we conclude that 50 to 75% of $N_0(E)$ is still a broadened Auger distribution. Thus R_t and hence b_i must be large enough for the Auger process to occur in a distance of the order of 1 Å when the ion is outside the surface. This distance and the ion velocity (22×10^6 cm/sec for 1000-eV, He^+ ions) give $R_t\sim2.2\times10^{15}$ sec^{-1} and $b_i(1000\text{ eV})\sim1.5$ eV. We may extrapolate these values linearly to zero velocity only if the barrier thins in such a way as to yield Eqs. (10) and (11) over the whole velocity range. This seems unlikely for reasons given below.

More light is cast on the relative magnitudes of b_i and b_n by the z' data of Fig. 10. For $K>100$ eV we cannot relate z' to broadening via Eq. (5) without first considering the broadening components which come into play in this region. We note that z', curve 1 of Fig. 10, rises less rapidly for $K>100$ eV than for $K<100$ eV. Since we expect b_n to continue to increase with increasing v this points to a leveling off of b_i caused by a collapse of the potential barrier between ion and solid over at least the top several eV of the filled band. z' as a measure of broadening will also be smaller than it should be for $K>100$ eV because in this range $N_0(E)$ shifts to lower energy as a result of decreasing effective ionization energy $E_i(s_t)$. It is possible to correct for this effect, however, using the results of earlier work[5] of fitting a theoretical $N_0(E)$ to the experimental distribution. This fit yielded the $E_i(s_t)$ values listed as $E_i'(s_m)$ in Table IV of Ref. 5, lines 5 to 9. These values of $E_i(s_t)$ are given here in Table IV. They are considered to be more trustworthy than is the reproduction of the form of the experimental $N_0(E)$ especially in the high-energy tail. Accurate theoretical reproduction of $N_0(E)$ requires that we know the true broadening function—a Gaussian was used in the earlier work. $E_i(s_t)$, on the other hand, is determined from the position of the high-energy side of $N_0(E)$ near its inflection point (approximately at half-maximum) and is very much less dependent on the choice of the broadening function.

Thus we are in a position to correct curve 1 of Fig. 10 by adding to each z' at the K in question the change in $E_i(s_t)$ from its value at 10 eV (Table IV). This assumes

TABLE III. Magnitudes of broadening components for He^+ ions.

	K eV	$v\times10^6$ cm sec^{-1}	(b_i+b_n) eV	b_i[a] eV	b_n[a] eV
Ge(111)	4	1.4	0.54	(0.33)	(0.17)
	70	5.9	2.2	(1.5)	(0.7)
	1000	21.9	4.2	(1.8)	(2.4)
Ni(111)	4	1.4	0.96	···	···
	70	5.9	2.9	···	···
GaAs(111)	4	1.4	0.37	···	···
	70	5.9	1.5	···	···
GaAs($\bar{1}\bar{1}\bar{1}$)	4	1.4	0.17	···	···
	70	5.9	0.6	···	···
GaAs(110)	4	1.4	0.31	···	···
	70	5.9	1.3	···	···

[a] Values for b_i and b_n were determined from the analysis of Fig. 10. That they are less certain than (b_i+b_n) is indicated by the parenthesis. b_n is an upper limit based on neglect of b_a and b_s for $K>100$ eV.

[20] H. D. Hagstrum, Y. Takeishi, G. E. Becker, and D. D. Pretzer, Surface Sci. 2, 26 (1964).

TABLE IV. Correction of z' for He^+ on Ge(111) from experiment 28 (Fig. 10).

K eV	$v\times10^6$ cm/sec	z'[a] eV	$E_i(s_t)$[b] eV	$\Delta E_i(s_t)$[c] eV	$z'+\lvert\Delta E_i(s_t)\rvert$ eV
10	2.2	1.1	22.4	0	1.1
33	4.0	1.9	22.2	−0.2	2.1
100	6.9	3.1	22.0	−0.4	3.5
333	12.6	3.7	21.5	−0.9	4.6
1000	21.9	4.3	20.5	−1.9	6.2

[a] Determined at $N_0(E)=1.5\times10^{-3}$ electrons/ion/eV from original data used to plot Fig. 11 of Ref. 3.
[b] Table IV, lines 5–9, Ref. 5. Here $E_i(s_t)\equiv E_i'(s_m)$ of the reference.
[c] Difference between $E_i(s_t)$ at K and at $K=10$ eV.

$E_i(s_t)$ has not changed much in the interval $K \leq 10$ eV as the data of Figs. 2 and 3 confirm. This procedure yields $z' + |\Delta E_i(s_t)|$ plotted as curve 2 of Fig. 10. Curve 2 may be used in Eq. (5) to obtain the sum of all velocity-dependent broadening components for $K > 100$ eV which will include b_i and b_n but may now also include contributions by b_a and b_s. This is the result of the fact that the correction of z' by $|\Delta E_i(s_t)|$ effectively shifts the $N_0(E)$ distribution so that it no longer moves on the E scale as K increases. Under these circumstances b_a and b_s, which increase with v, will contribute to z'. This accentuates the evidence that b_i levels off for $K > 100$ eV but makes separation of components more difficult. If we neglect b_a and b_s we may draw a line (curve 4 in Fig. 10) through the origin parallel to the high-energy portion of curve 2 giving the equivalent z' values as an upper limit of b_n. b_i is then the difference between curves 2 and 4 and is seen to rise linearly for $K > 100$ eV and level off to a more or less constant value for $K > 100$ eV. The values of b_i and b_n for $He^+/Ge(111)$ in Table III are calculated on the above assumption. b_i shows Auger neutralization to be a fast process having a rate of 5×10^{14} sec^{-1} for 4-eV He^+ ions on Ge(111). The maximum transition rate from b_i is about that required for the process to occur with appreciable intensity for 1000-eV ions. By Eq. (14) the values of b_n specify a reasonable value of ~ 0.5 Å for d.

The data of Figs. 8 and 9 and Table I indicate that the magnitude of $(b_i + b_n)$ for $K < 100$ eV depends on both the ion and the solid used. $(b_i + b_n)$ is generally lower for the semiconductors than for the one single crystal metal studied and covers a range of 5 to 1 from Ni(111) to GaAs($\bar{1}\bar{1}\bar{1}$). It would not be surprising if both b_i and b_n were specific to the ion-target combination. A complete interpretation of the experimental results is not now possible but suggestions of possible contributing factors can be made.

Since all ions are neutralized outside the surface we expect by Eq. (10) that b_i will depend on the rate of rise of $R_t(s)$ with decreasing distance specified by the parameter a of Eq. (7). This could certainly vary with ion-target combination but is probably not as sensitive as is b_n for reasons we shall now enumerate. At the end of Sec. III we indicated that b_n will depend not only on ion velocity but on the density and character of the final states into which electrons from the solid are excited nonadiabatically. For metals we expect the largest density of final states for this process and hence the largest $(b_i + b_n)$ as is observed. For semiconductors the only final states available are surface states and the excited levels in the atom itself. The probability of filling of these excited states is determined by how far they lie above the Fermi level of the solid. We thus have a complicated dependence on characteristics of the solid (work function for metals, electron affinity, band gap, and density of surface states for semiconductors) and characteristics of the atom (position of excited levels). Excited levels relative to the vacuum level lie lowest for Ne, next lowest for He, and highest for Ar (Fig. 24 of Ref. 4). Thus we expect b_n to decrease from Ne to He to Ar. This ordering in the magnitude of $(b_i + b_n)$ is observed only for the metal nickel. Why $(b_i + b_n)$ for Ar is greater than for He in the cases of the semiconductors is not understood.

That the excited atomic states play a role in the Auger process for Ne^+ is also suggested by the anomalous behavior of the total yield with increasing ion energy.[4,5,8] Excitation into excited atomic states can produce a more rapid extension of the high-energy tail of the Ne^+ distribution than would simple convolution by a wider broadening function. Thus there would be more extension to high energy than is consistent with the general smearing of the distribution and z' used in Eq. (5) will overestimate the broadening parameter. Thus $(b_i + b_n)$ calculated by Eq. (15) from the data of Table I is in all probability too large for Ne^+. This conclusion is consistent with the anomalous behavior for Ne^+ of the total electron yield with incident-ion energy.[1,3,6] It is most likely an oversimplication to assume that all the characteristics of "broadening," defined so loosely as to include the effect of excited atomic states, are representable by a simple convolution.

On the above picture z' for semiconductors should also depend on the photothreshold Φ. Larger Φ requires larger nonadiabatic excitation to reach the excited atomic states. The data of Gobeli and Allen[21] give Φ as 5.47 eV for GaAs(110), 4.80 eV for Ge(111) and would thus require z' for Ge(111) to be greater than that for GaAs(110) as is observed.

IV. BARRIER BETWEEN ION AND SOLID

The conclusions we have drawn above concerning initial-state lifetime broadening b_i and the corresponding total transition rate $R_t(s_t)$ tell us something about the barrier between ion and solid when the Auger process occurs and how it changes with ion velocity. Our interpretation of the observed broadening calls for a barrier which thins with increasing v in the range $K < 100$ eV and has essentially collapsed at $K \sim 100$ eV leaving $R_t(s_t)$ roughly constant for $K > 100$ eV. $R_t(s_t)$ will, of course, eventually fall when the ion velocity becomes sufficiently large to reduce the available time for the Auger process to occur outside the surface.

A further conclusion from the experimental $N_0(E)$ distributions also bears on the nature of the barrier. As can be seen in Figs. 2 and 3, $N_0(E)$ varies with increasing K, at least in its higher energy portions, as though it were derivable by convoluting an "unbroadened" distribution by a broadening function of increasing breadth [Eq. (1)] coupled with a general reduction in its magnitude. A simple convolution would, for example, blunt the peak at $E \cong 8$ eV in Fig. 3 and fill in the valley at $E \cong 6$ eV. These observations are

[21] G. W. Gobeli and F. G. Allen, Phys. Rev. (to be published).

interpreted to mean that no drastic change occurs in the variation of transition rate with band energy for the participating electrons as the barrier thins and the over-all rate increases.

The magnitude of the barrier between ion and solid is important in the Auger neutralization process because it controls the tunneling probability of electron 1 from the solid into the ground state of the incoming ion (Fig. 1). In previous work[4,5,10] it has been shown that the magnitude of the matrix elements of the process depends on the magnitude of the wave function of electron 1 in the vicinity of the atomic ground state. Barrier penetration will in general be expected to depend on the energy level of electron 1. Electron 2 is affected by barrier penetration only if the range of the matrix element is small and electron 2 is excited only at or near the surface.

We now consider what we expect the variation of a differential rate function $R_\zeta(\zeta,s)$ to be for different ion-solid separations. $R_\zeta(\zeta,s_t)$ is defined such that $R_\zeta(\zeta,s_t)d\zeta$ is the transition rate for those processes, occurring with the ion at the distance s_t in which electron 1 is drawn from an initial state in the solid lying in an energy element $d\zeta$ at the energy ζ. ζ, as indicated in Fig. 1, is the energy in the filled band of the solid measured down into the band from its top. The total transition rate for all processes with ion-solid distance equal to s_t is $R_t(s_t)=\int_0^{\zeta_0} R_\zeta(\zeta,s_t)d\zeta$. Here ζ_0 is the energy at the bottom of the filled band. $R_\zeta(\zeta,s_t)$ may, of course, fall to zero before ζ_0 is reached.

In Fig. 13 we have plotted schematically how $R_\zeta(\zeta,s)$ is expected to vary for several ion-solid separations. For large separation, curve 1, $R_\zeta(\zeta,s)$ is small and limited to the top of the band. Electron 1 must then come from the top of the band while electron 2 may be drawn from anywhere in the band. Neglecting other possible energy variations of the matrix element the kinetic-energy distribution of excited electrons will then be determined by the initial-state density of electron 2 only. Thus the process, although involving two electrons, is essentially a one-electron process as far as variation with energy over the band is concerned and resembles the Auger de-excitation of an excited atom.[4] We shall call this the "distant" or "one-electron" limit or regime of the Auger neutralization process.[22]

As s decreases, $R_\zeta(\zeta,s)$ increases in magnitude and extends deeper into the band. It also shows a decrease in the rate of variation with ζ near the top of the band, and tends toward independence of ζ, curve 5, when the barrier has completely collapsed. This we might call the "close" or "two-electron" limit of the process. In this limit the kinetic-energy distribution of the excited electrons, by virtue of variation of both initial states over the band, will involve the integral self-convolution of the state density in the filled band.[4,5]

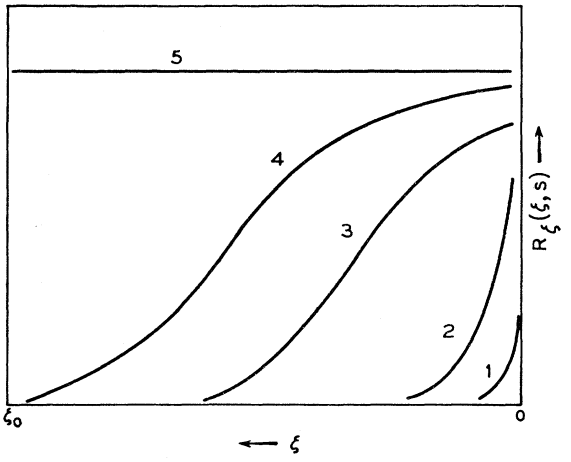

FIG. 13. Schematic representation of the differential rate function $R_\zeta(\zeta,s)$ as a function of ζ for Auger processes occurring at different distances from the surface. Curve 1 is for processes occurring far from the surface where the barrier is thick. The remaining curves in sequence are for decreasing distances ending with curve 5 which represents the condition for a completely collapsed barrier between ion and solid.

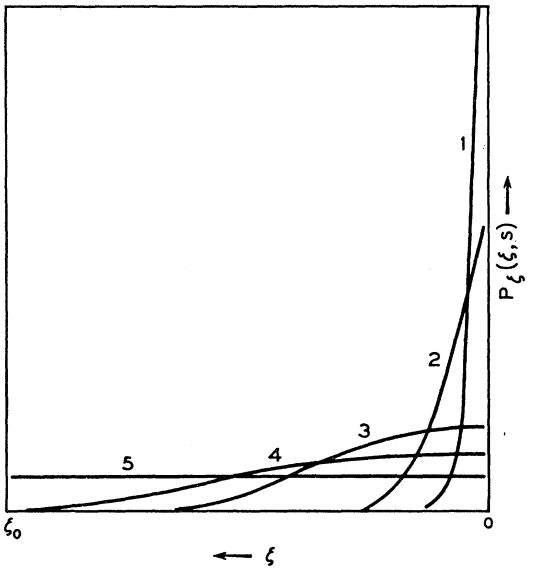

FIG. 14. Schematic representation of the relative probability function $P_\zeta(\zeta,s)$ as a function ζ for Auger processes occurring at different distances from the surface. These curves are derived from those for $R_\zeta(\zeta,s)$ in Fig. 13.

There is good evidence that for the slower ions ($K<100$ eV) all ions are neutralized before striking the surface.[4,5] Thus we may think of the variation of transition rate with the energy ζ of electron 1 in terms of a relative probability function $P_\zeta(\zeta,s)$ defined such that $P_\zeta(\zeta,s_t)d\zeta$ is the relative probability that electron 1 tunnels from an initial level lying in $d\zeta$ at ζ in a transition occurring when the ion is at s_t. Here $P_\zeta(\zeta,s_t)$ has the same form as $R_\zeta(\zeta,s_t)$ but is normalized such that $\int_0^{\zeta_0} P_\zeta(\zeta,s_t)d\zeta=1$. P_ζ curves derived from the

[22] D. Sternberg, Ph.D. thesis, Columbia University, 1957 (unpublished).

schematic R_ζ of Fig. 13 are shown in Fig. 14. We emphasize that in the actual situation of an ion fired at a surface, normalization of P_ζ holds only for the lower ion velocities where all ions undergo Auger neutralization before striking the surface.

We would like to know where we stand among the possibilities depicted in Fig. 14. The conclusion that the $N_0(E)$ variation with K varies as a convolution coupled with a drop in magnitude indicates that the appropriate P_ζ function resembles curves 3 or 4 of Fig. 14 and not curves 1 or 2. This places us near the "collapsed barrier" or "two-electron" limit for the process. This further agrees with our conclusion that total $R_t(s_t)$ does not increase appreciably above $K\sim 100$ eV. The drop in P_ζ as K increases, which results from thinning of the barrier further down in the band and the consequent increase in the Auger probability for lower lying band electrons, would then be called upon to explain the decrease in magnitude of the higher energy portions of $N_0(E)$ with energy K. If the barrier were thick and P_ζ were a rapidly varying function like curves 1 or 2 of Fig. 14 we would expect the shape of $N_0(E)$ to be affected by the shape of P_ζ and that this effect would be velocity sensitive contrary to what is observed.

Further evidence pointing to a thin or essentially nonexistent barrier over the top several electron volts of the filled band comes from one-dimensional calculations of the barrier itself. Arguments based principally on the fact that the effective neutralization energy of the ion when the Auger process occurs is 1.6 to 2.0 eV less than the free-space value make it highly probable that the ion-solid separation is then in the range 2 to 3 Å.[4,5] One-dimensional barriers calculated for separations of 2.2 and 3.0 Å are shown in Fig. 15. Curves 1 and 2 are calculated from the potential, given by Propst,[10] made up of the Coulomb potentials of the ion, the image of the ion, and the image of the electron. Propst's potential is adjusted so that the barrier comes to the *top* of the filled band at the solid surface ($x=0$). Curves 3 and 4 are plots of the function

$$V(x)=-3.6\left(\frac{1}{x}-\frac{0.09}{x^2}+\frac{8x}{5^2-x^2}\right) \qquad (16)$$

obtained by combining the surface barrier derived by Cutler and Gibbons[23] for the periodic deviations from the Schottky line with the same image potentials used by Propst. It is probable that Propst's potential gives a one-dimensional barrier which is too thick because of the stipulation that $V(x)=-\varphi$ at $x=0$. Even though one-dimensional calculations underestimate the thickness of the true barrier in three dimensions they do support the contention that the barrier is thin. In three dimensions the tunneling probability can increase at energies above the barrier maximum or saddle point as this point moves to lower energies. This occurs because the "width" of the accessible opening into the atomic well increases as the saddle point moves down. Thus one can have a situation in three dimensions where the differential transition rate can increase over the top part of the band without introducing a drastic variation with energy in this region. Extrapolation to $v=0$ of data taken in this velocity region should give the magnitude of the velocity-dependent broadening components *in this velocity region*. This is true despite the fact that an actual experiment with slower and slower ions would bring in new effects as the barrier thickens.

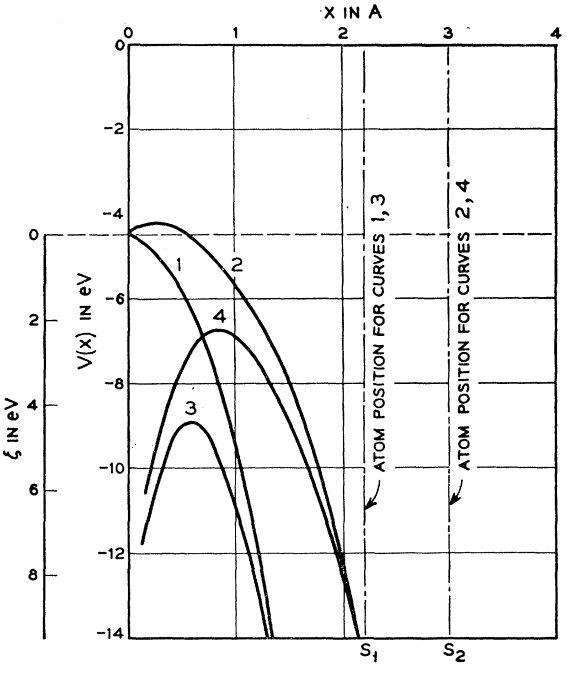

FIG. 15. Plots of one-dimensional potential barriers $V(x)$ between ion and solid calculated by two formulas for two ion-solid separations s_1 and s_2. Curves 1 and 2 are for Propst's potential, curves 3 and 4 for a potential combining the barrier of Cutler and Gibbons with ion and electron image potentials. Curves 1 and 3 are for $s=2.2A$, curves 2 and 4 for $s=3.0A$.

Other reasons for believing that we are not at the thick barrier or one-electron limit are the following: (1) The high-energy tail of the $N_0(E)$ distribution resembles the self-convolution of the band-state density distribution as demanded by a two-electron process and does not resemble the density distribution itself as in a one-electron process. In a semiconductor the state density in the valence band varies with energy distance from the top of the band ζ as $\zeta^{1/2}$. The integral self-convolution of the valence-band function varies as ζ^2. The $N_0(E)$ distributions of Figs. 2 and 3 vary with energy measured from the high-energy limit E_m more like $(E_m-E)^2$ than like $(E_m-E)^{1/2}$. (2) Comparison of Auger yields for He^+ and Xe^+ ions on metals and semiconductors are made in Table V. Note that $\gamma_i(He^+)/\gamma_i(Xe^+)$ is much larger for the semiconductors than for the metals. We expect the much wider filled

[23] P. H. Cutler and J. J. Gibbons, Phys. Rev. **111**, 394 (1958).

TABLE V. Total electron yields for 10-eV, He^+ and Xe^+ ions on metals and semiconductors.[a]

Target	$\gamma_i(He^+)$	$\gamma_i(Xe^+)$	$\gamma_i(He^+)/\gamma_i(Xe^+)$
W	0.289	0.013	22
Mo	0.300	0.022	14
Ge(111)	0.196	0.0006	326
Si(100)	0.172	0.0005	344

[a] The γ_i values are taken from Table I of Ref. 3 in which results for metals and semiconductors are summarized.

bands in the semiconductors to present filled electronic levels to the empty ground state of the incoming Xe whereas the narrower metal bands lie entirely above the Xe ground state. Thus resonance neutralization of Xe^+ is possible for the semiconductors and not for the metals. Interpreted in this way, and no satisfactory alternative is apparent, the results of Table I indicate that the barrier is thin enough for resonance neutralization at a level some 10 eV or more below the vacuum level to compete successfully with Auger neutralization involving electrons much higher in the band. (3) The total transmission rate for $K\sim4$ eV must be of the order of 5×10^{15} sec^{-1} corresponding to $b_i\sim0.33$ eV [Table I for He^+/Ge(111)]. This makes Auger neutralization a very fast radiationless process and leaves little room for any reduction in rate caused by a thick barrier. Autoionization and predissociation in molecules obliterate rotational structure but not vibrational structure and thus have rates less than 4×10^{14} sec^{-1} (broadening 0.25 eV).[24] Similar or somewhat larger rates are found for autoionizing atomic levels from both experiment and theory.[25]

[24] G. Herzberg, *Spectra of Diatomic Molecules* (D. Van Nostrand Company, Inc., New York, 1950), 2nd ed., pp. 409 ff. and 414.
[25] W. Finkelnburg and Th. Peters, *Handbuch der Physik*, edited by S. Flügge (Springer-Verlag, Berlin, 1957), p. 115.

VI. CONCLUSIONS

It has been shown that energy broadening in the Auger neutralization process varies linearly with velocity for slower ions, generally for ion energies less than 100 eV. The rate of increase of broadening diminishes above 100 eV. Magnitudes have been derived from the experimental data on the basis of a plausible extrapolation out of the velocity range available. Broadening has been shown to be specific to the ion and solid employed.

The firmest interpretative conclusion is that for slow ions the broadening is the sum of two components due to initial-state lifetime and nonadiabatic excitation. Numerical estimates of the relative magnitudes of these components have been given. It is concluded that the barrier between ion and solid is thin for slow ions and has essentially collapsed for electrons over the top several electron volts of the filled band at ion energies above 100 eV. Thus we should expect that we are near the "two-electron" limit at which the kinetic-energy distribution is an integral fold of the state density distribution in the filled band of the solid.

The suggestion has been made that the variations of experimental broadening from ion to ion and solid to solid have to do principally with the probability of nonadiabatic excitation which varies with energy separation of the energy levels in the solid and the excited states of the atom.

ACKNOWLEDGMENTS

It is a pleasure to acknowledge discussions with several of our colleagues, in particular C. Herring, who suggested the possibility of nonadiabatic excitation, E. O. Kane, and P. A. Wolff.